Dalton Transactions

An international journal of inorganic chemistry

rsc.li/dalton

Volume 46
Number 10
14 March 2017
Pages 3073-3412

ISSN 0306-0012

COMMUNICATION
Douglas W. Stephan et al
N-Heterocyclic carbene stabilized parent sulfenyl, selenenyl, and tellurenyl cations (XH+; X = S, Se, Te)

ROYAL SOCIETY OF CHEMISTRY

This is an Accepted Manuscript, which has been through the Royal Society of Chemistry peer review process and has been accepted for publication.

Accepted Manuscripts are published online shortly after acceptance, before technical editing, formatting and proof reading. Using this free service, authors can make their results available to the community, in citable form, before we publish the edited article. We will replace this Accepted Manuscript with the edited and formatted Advance Article as soon as it is available.

You can find more information about Accepted Manuscripts in the Information for Authors.

ROYAL SOCIETY OF CHEMISTRY

rsc.li/dalton

Metal organic framework top-down and bottom-up patterning techniques

César L. Ruiz-Zambrana,[1,2] Magdalena Malankowska,[1,2] Joaquín Coronas[1,2,*]

[1]Instituto de Nanociencia y Materiales de Aragón (INMA), Universidad de Zaragoza-CSIC, 50018 Zaragoza. Spain

[2]Chemical and Environmental Engineering Department, Universidad de Zaragoza, 50018 Zaragoza. Spain

[*]Corresponding author e-mail address: coronas@unizar.es

**Abstract**

Metal organic frameworks (MOFs) have recently attracted considerable research interest in several fields from coordination chemistry and materials science to engineering and medicine due to energy and environmental issues but also to the need of new paradigms of efficiency and sustainability according to the requirements of the XXI century global society. Because of their crystalline and organic-inorganic nature, they are able to crystallize constituting intergrown architectures ductile enough as to be patterned, with the use of the appropriate techniques, as nano- and micro-devices with multiple applications. This review comprehensively summarizes the recent state of the art in the use of top-down and bottom-up methodologies to create MOF structures with a defined pattern at the nano- and micro-scale.

## 1. Introduction

Metal-organic frameworks (MOFs) are a growing class of porous and crystalline hybrid (organic-inorganic) materials. They are characterized by high porosity and surface area as well as flexibility in pore shape and size and atomic structure.[1] Since MOFs are formed by self-assembly of complex subunits that consist of transition metal centres interconnected by organic ligands, they show good interaction with polymers, thus they are commonly used in the preparation of mixed matrix membranes (MMMs) especially

for gas separation.[2,3] However, gas separation through MMMs is not the only application of MOFs. They also show promising performances in energy production[4], catalysis[5], bioreactors[6], diagnostics and controlled drug release[7], solar cells[8], sensors[9], microelectronics[10], optics,[11] among others. Moreover, incorporation of MOFs into microfluidic devices or miniaturized chips, such as lab-on-a-chip, gains more and more attention.[6] The microfluidic devices for various applications present novel chemical, optical, mechanical, magnetic, medical or diagnostic properties with better performance in comparison to their macro counterparts emphasizing the need of miniaturisation.[12]

All these applications require excellent and precise control of the position of the functional material. Controlled location technology allows not only to avoid MOF agglomeration (as it is a common problem to avoid in membrane preparation) but it also favours the fabrication of very thin MOF layers with defined geometry and structure. This also would allow procedures involving the minimum amount of the MOF active material needed to enhance a certain separation performance, as demonstrated from simple dip-coating[13] or through the use of Langmuir-Schaefer technique.[14] The main challenge apart from process optimization (synthesis of the desired functional material) is an integration of the material into a useful platform.[15] Moreover, the controlled thickness and shape of MOF layers as well as their interaction with various supports are of great interest for the applications mentioned above. Another interesting feature that can be affected by the surface morphology is the surface property in terms of hydrophilicity and hydrophobicity. According to the Wenzel equation, a hydrophilic material surface can become more hydrophilic as a result of roughness increase[16], and the same operates for a hydrophobic surface. There are many different patterning techniques that in combination with surface modification enable high control in the location process of MOF. In this context, MOF patterning can be divided into bottom-up and top-down patterning approaches. In this review, we will describe both: the bottom-up and top-down patterning techniques; however, we will give a more detailed explanation about the current technologies that are part of a top-down strategy, focussing more on the coating and membrane strategies of synthesis involved in MOF patterning processes than on the general methodologies to obtain those coatings or to synthesis MOFs. Table 1 is intended to give a general overview of the main advantages that the patterning techniques may bring to MOFs.

**Table 1.** Advantages of MOF patterning and their qualitative expression.

| Advantage | Expression |
|---|---|
| Avoidance of agglomeration | Favouring interaction with other components of the device |
| Control of MOF thickness | Homogenization of local properties |
| Control of MOF location and architecture | Maximizing active specific area and creating micro- and nano-devices with high precision |
| Modification of surface properties | Hydrophilicity and hydrophobicity can be enhanced by increasing roughness |
| Minimization of use of active material | Reducing costs and facilitating implementation |
| Multifunctionality | Devices with simultaneous reaction and separation properties (both intrinsic of MOFs) |

## 2. Patterning techniques

Controlled location technology enables to design and envision the MOF coatings focusing on homogenous thin films as well as on a permanent MOF attachment to the substrate. It has to be taken into account that to fully control the properties of a MOF thin film some important features have to be considered such as: crystal alignment (in-plane and out-of plane orientations), film roughness, lattice interpenetration, crystal size and density, and domain size and adhesion to the substrate. There are different MOF spatial configurations that have to be considered when choosing the proper technique for the MOF controlled location such as: 1D arrangement (direction perpendicular to the plane), 2D (in the plane) or 3D configuration (space).[12] Different patterning approaches can be distinguished for 2D or 3D growth: bottom-up and top-down.
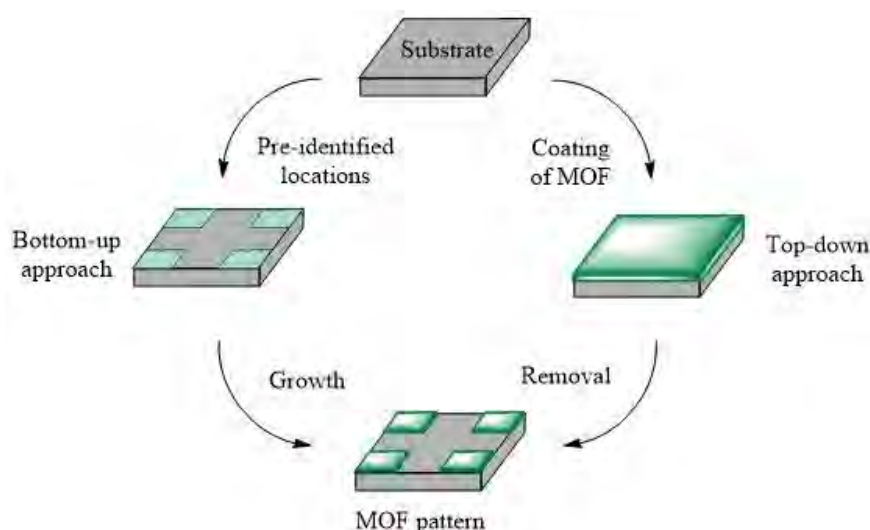
**Fig. 1** Different methodologies to design MOF patterns: bottom-up and top-down approaches.

Bottom-up approach is defined as the direct growth of MOF in pre-identified locations, while in the top-down technique the spatial control of porous crystals is achieved by either transferring or removal of pre-existing MOF crystals or continuous layers of intergrown MOF crystals (Fig. 1).[12]

### 2.1. Bottom-up MOF patterning

**Table 2**. Bottom-up techniques for MOF patterning.

| Technique | MOF | Resolution | Substrate | Reference |
|---|---|---|---|---|
| Liquid-phase epitaxy | $Cu_2(ndc)_2(dabco)$ | µm range | Au templates | [17] |
| Nanografting by atomic force microscopy (AFM) | $[Cu_3(BTC)_2]^*$ | ~ 15 µm | Au coated substrate | [18] |
| Microfluidics | $[Cu_3(BTC)_2]$ | µm range | Glass wafer with a thin layer of indium tin oxide (ITO) | [19] |
| Electrochemical deposition | $[Cu_3(BTC)_2]$ | ~ 20 µm | Glass treated with chlorotrimethylsilane | [20] |
| Electrophoretic deposition | NU-1000 | ~ 25 µm | Fluorine-doped tin oxide (FTO) | [21] |
| Contact printing | $[Cu_3(BTC)_2]$ | µm range | Glass | [22] |

| | MOF-5, IRMOF-10 and IRMOF-9 | ~ 10 µm | Silicon wafer | 23 |
|---|---|---|---|---|
| Pen-type lithography | [Cu$_3$(BTC)$_2$] | µm range | Alkanethiol-modified gold surfaces. | 24 |
| Chemical vapour deposition | ZIF-8 | µm range | Silicon wafer | 25 |
| Nucleating agents | MOF-5 | ~ 5 µm | Silicon wafer | 26 |
| Laser radiation | ZIF-8 | µm range | Brass | 27 |
| | MIL-100(Fe) and FeBTC | µm range | Glass | 28 |
| Spray coating | [Cu$_3$(BTC)$_2$] | µm range | Au coated substrate | 29 |
| Ink-jet printing | [Cu$_3$(BTC)$_2$] | µm range | Plastic, paper and textile substrates | 30 |
| | MOF-525 | µm range | ITO | 31 |

*[Cu$_3$(BTC)$_2$] is commonly known as HKUST-1.

Variety of strategies are used in the bottom-up protocols to control the location of MOF in the self-assembly route. Besides the conventional techniques of direct crystallization and secondary growth (from a previous seeding to hinder homogeneous nucleation), some of the most important procedures include: surface functionalization by micropatterning, microfluidics, electrochemical deposition, contact printing, chemical vapour deposition, nucleating agents and ink-jet and spray coatings (see Table 2).

Surface functionalisation in combination with other techniques is one of the most effective ways to pattern MOFs. It can be compared to some sort of substrate preparation for the MOF attachment, thus the functionalised surface should promote growth and nucleation of MOF on top of it.[12,32] Surface functionalisation can be achieved through, for example: i) liquid-phase epitaxy (LPE)[32] which is *in situ* crystallization, ii) microcontact printing (µCP) where the substrate functionalisation can be precisely controlled, or iii) layer-by-layer (LbL) technique where the self-assembly monolayer (SAM) is alternately immersed under the organic linker and metal precursor solutions with washing steps in between.[12] Once the SAM layer is prepared by a well-established technique a MOF can be patterned, for example, *via* nanoshaving or nanografting where atomic force microscopy (AFM) is used to laterally pattern the layer with the resolution of a few nanometers.[18,33]

Next patterning technique that is gaining more and more attention is microfluidics. Microfluidic devices enable a fine control and precise manipulation of the reactions that take place inside the microfluidic channels. Moreover, microfluidics offers unique conditions in comparison to their bigger counterparts such as: large surface to volume ratio, turbulence-free environment working on laminar flow, ability to use small volumes and their precise control and manipulation as well as outstanding control over heat and mass transport.[34] Moreover, microfluidic lab-on-a-chip devices provide precise control of the materials introduced in the system as well as a close imitation of the natural human organ. One of the techniques that is suitable for MOF patterning is digital microfluidics. This technique possesses a number of advantages over other technologies: i) it allows patterning of MOFs on a wide range of substrates, ii) it enables high level of control over mixing and fluid dispensing, and iii) small droplets (<1 μL) can be independently manipulated and controlled thanks to the software providing electronic signals (Fig. 2).[19]
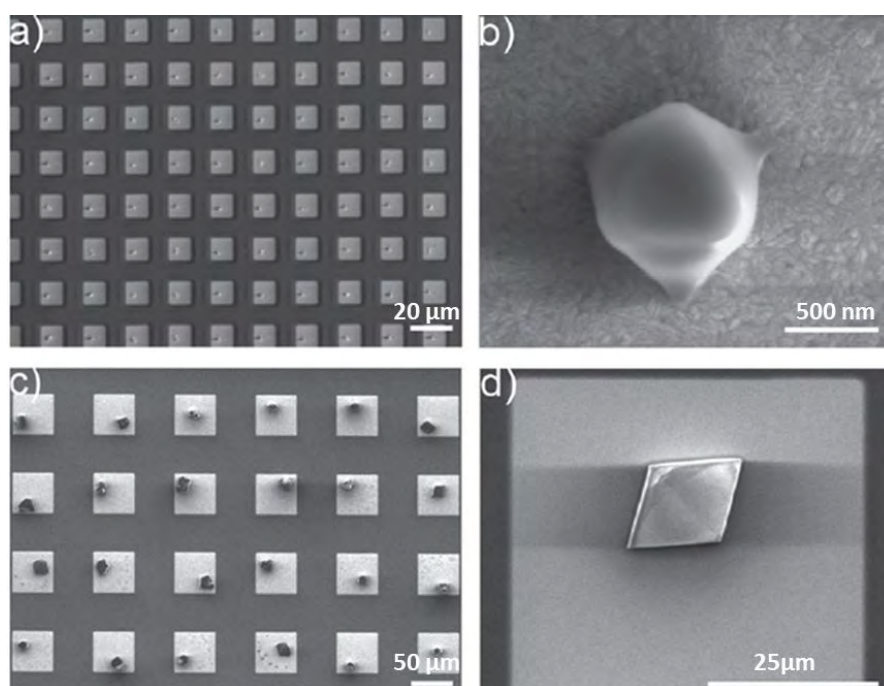


**Fig. 2** SEM images of a) crystalline HKUST-1 in square micropatches with a 10 μm × 10 μm geometry, and b) frontal view of a single HKUST-1 crystal. c) Single HKUST-1 crystals in micropatches of 50 μm × 50 μm, and d) frontal view of a rhombohedral HKUST-1 crystal. Reproduced from Ref.[19] with permission from [John Wiley and Sons], copyright [2012].

Microfluidic devices could be used for solvothermal MOF crystallization process due to the advantages over conventional solvothermal methods such as: increased ability to control crystallization and narrow particle size distribution, increased reaction kinetics

and enhanced process efficiency.[12,35] An additional advantage of MOF-focused microfluidics, not yet realised in the context of this revision, relays on the possibility of carrying out sequential chemical modifications of MOFs by pumping a secondary solution including some chemical able to react with the MOF functional groups, as is the case of the transformation of zeolitic imidazolate framework (ZIF) ZIF-94 into ZIF-93 by reaction with amine.[36]

Electrochemical deposition is another technique for MOF thin film synthesis and it includes anodic and cathodic deposition for synthesised MOF coatings.[37] A uniform coating with crystal sizes ranging from 0.5 to 5 μm is produced due to the MOF crystal nucleation and growth close to the surface of the substrate. This happens when the anode, that is formed with the desired metal to synthesize the MOF, starts to dissolve due to the positive voltage that is applied to the electrochemical cell. The process of anode dissolution releases metal ions into the solution where they react with the ligand and produce MOF concentrated near the anode. Anodes of Cu, Fe, or Zn have been widely used in this technique.[15] However, it is important to clarify that there are some metals that cannot be used in anodic deposition because they are susceptible to corrosion.[38] In case of the cathodic deposition, the solution that already consists of bridging ligands and metal ions is used for the suspension of the substrate to be coated. In this case the substrate acts as the cathode of the cell. The function of the cathode is to release electrons. It produces a local area with basic properties close to the cathode, favouring the deprotonation of the ligands. This favours the reaction of these with the metallic ions to generate the desired MOFs on the cathode surface. Electrochemical deposition technique to generate MOF patterns is based on the use of lithographed metals as anode and cathode. In this way, the morphology of the metals is replicated in the MOFs when they are deposited. An example was provided by Abeloot *et al*.[20] These authors demonstrated that the methodology used offers an advance in MOF processing for applications such as sensors and other thin film devices. In this research, a glass slide treated with chlorotrimethylsilane was covered with metallic copper forming a pattern of squares of 50 μm × 50 μm. Later, octahedral $[Cu_3(BTC)_2]$ (MOF commonly known as HKUST-1) crystals of about 100-200 nm were deposited on the metal adopting the same architecture.

Contact printing combined with evaporation induced growth (also known as evaporation induced self-assembly, EISA) is another methodology that can be used to directly produce high quality patterns of MOF crystals. In this approach, a MOF precursor solution is used

to wet the microlithographed stamp which are usually made from polydimethylsiloxane (PDMS). The stamp is then placed in contact with the substrate. The MOF precursor is enclosed below the stamp geometry due to capillary forces and subsequently its growth is limited to specific areas. Next, the substrate is heated up to 100 °C, and hence the solvent starts to evaporate which results in the MOF nucleation and growth in an ordered manner (Fig. 3).[22]
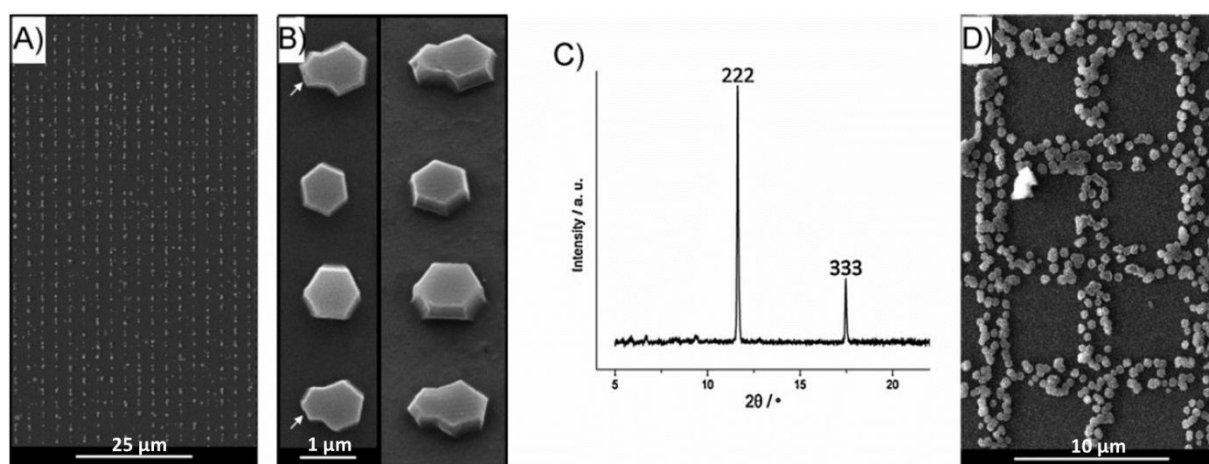


**Fig. 3** a) SEM images of crystalline HKUST-1, b) frontal view of single HKUST-1 crystals (left) and at 35° angle (right), different growths caused by second nucleation are pointed out. c) XRD reflection pattern of HKUST-1 showing preferential crystallographic orientation, and d) negative replica to the previous HKUST-1 in a). Reproduced from Ref.[22] with permission from [John Wiley and Sons], copyright [2010].

Moreover, the use of pen-type nanolithography for patterning MOF crystals was reported as well.[24] In this case the chosen MOF was also HKUST-1 that worked as a stable precursor and dimethyl sulfoxide (DMSO) was used as a solvent. It was concluded that the hydrophobicity and hydrophilicity of the surface play a critical role in obtaining controlled MOF crystallization per droplet. The authors found that if the surface was coated with hydrophobic functional groups, the contact angle increased and a single crystal with approximate edge dimensions of 550 nm was obtained. However, if the surface was hydrophilic and as a result the substrate was wetted by the solution, multiple small crystals with edge dimensions from 300 to 750 nm were formed.[24] This technique generates new opportunities to integrate MOFs in specific areas with high control and the authors expected the prepared materials to have an important impact on sensors, magnetic and electronic devices.

Chemical vapour deposition (CVD) has been widely used to coat on desired substrates. In general, CVD includes two steps: first the adsorption of the volatile precursors onto the substrate, and then the reaction of these precursors onto the platform surface. Inspired by this technique, Stassen *et al.*[25] introduced the concept of MOF-CVD, in which metal oxides are deposited in the substrate, and then these precursors are transformed into MOFs in a vapour–solid reaction. The development of this technique could have great impact on the use of MOFs in microelectronics. Moreover, the use of this methodology to generate MOF patterns has been recently explored.[39] An example was reported by Stassin *et al.*[40] In this work, the authors developed patterned Cu-based MOF. They used a shadow mask to deposit the metal oxide (CuO) in pre-identify regions. Once the metal oxide pattern was formed, the reaction with the dicarboxylic acid linker vapour produced the MOF.

The use of nucleating agents is another technique where MOF is grown and patterned in a controlled way. This occurs thanks to the seeding procedure where the nucleation of MOF is induced on specific particles or substrates. There are different types of "seeds" for MOF growth: i) heterogeneous seeds that are different materials that promote the formation of MOF,[41] or ii) homogenous seeds that possess the same MOF chemistry and structure as the one that will be grown.[42] Lithographed patterned wells with a diameter between 30 µm and 50 µm and a depth of 100 µm were used to spatially locate the MOF growth by positioning isolated microparticles inside them.[26] Also, regularly distributed laser perforations carried out on a metal (brass) sheet were filled with intergrown ZIF-8 giving rise to 20-30 µm diameter micromembranes able to separate the $H_2/CH_4$ mixture (Fig. 4).[27] In this case, the control of the Nd:YAG laser operating conditions allowed for the drilling of the 75 µm thick brass sheets generating porosities in the 1.6-18% range. In a subsequent stage, the perforated supports were submitted to solvothermal synthesis of ZIF-8, which was incorporated not only on the support surface but also inside its holes with some degree of preferential crystallographic orientation of the [100] planes parallel to the metal sheet.
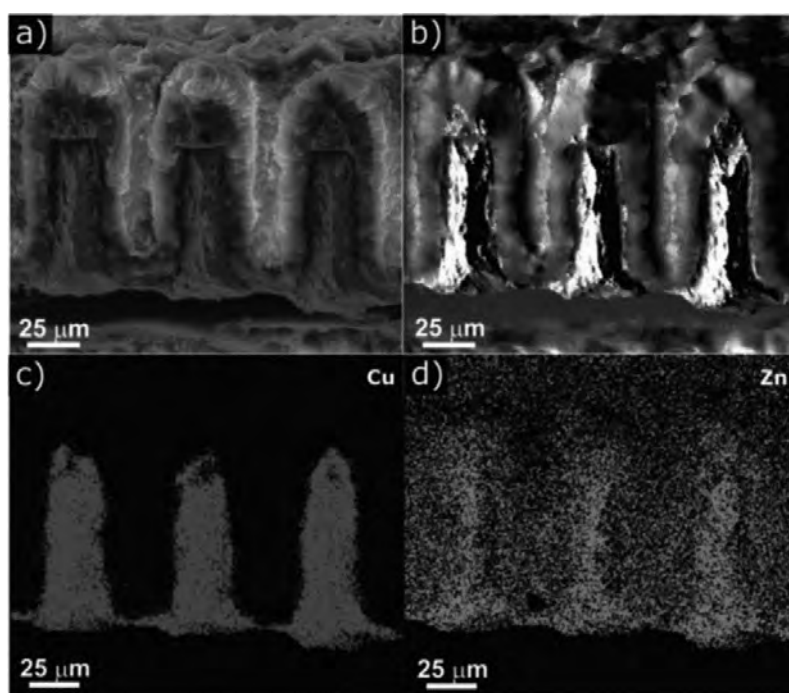
**Fig. 4** Cross-section of ZIF-8 micromembrane: a) SEM image where irradiation occurs from top to bottom of the membrane, b) backscattering SEM image; (c and d) Cu and Zn, respectively, EDX mapping of the same previous images. Reproduced from Ref. [27] with permission from [The Royal Society of Chemistry], copyright [2014].

Ink-jet and spray coatings are two techniques that allow the production of MOF patterns over large areas (from 10 cm$^2$ to 1 m$^2$).[30] In case of ink-jet coating it was shown that large patterns of MOF can be printed onto flexible substrates such as paper, textile fabrics or plastic, thanks to the adaptation of a standard office ink-jet printer.[30] For the spray coating it was reported that it can automate the LbL process. The authors aimed for growing of well orientated HKUST-1 films on the Au substrates that were initially patterned by μCP. The substrates were alternately sprayed with two different metal and ligand solutions with controlled time (10 and 20 s, respectively). The developed MOF micropatches of about 4.5 μm × 4.5 μm were uniform, well orientated and they maintained the geometry of SAM that was micro patterned on the substrate. Moreover, it is expected that these MOF-based materials have application in membrane technology.[29]

## 2.2. Top-down MOF patterning

**Table 3**. Top-down techniques for MOF patterning.

| Technique | MOF | Resolution | Substrate | Photoresist | Reference |
|-----------|-----|------------|-----------|-------------|-----------|

**Dalton Transactions Accepted Manuscript**

| Deep X-ray lithography | ZIF-9 | 25 µm | Silicon wafer | PhTES | 43 |
|---|---|---|---|---|---|
| UV-lithography | ZIF-8 | µm range | Silicon wafer | AZ1815 | 44 |
| | SURMOF [Zn(N$_3$-BPDC)$_2$(dabco)] | µm range | Au- substrate | SURMOF | 45 |
| UV-lithography and imprinting | NH$_2$-MIL-53(Al), ZIF-8 and ZIF-67 | 5 µm | Al$_2$O$_3$, SiN, SiO$_2$, silicon, ITO, Au, Ti, Ni, Cu, Al, and PMMA | SU-8 | 6 |
| Soft nanoimprinting lithography | ZIF-8 | ~ 200 nm | Silicon, flexible plastics, and aluminium | - | 46 |
| Electron beam lithography | ZIF-L, MIL-101(Cr), ZIF-8 and Zn(BeIm)OAc | µm range | Silicon wafer | ZIF-L, MIL-101(Cr), ZIF-8 and Zn(BeIm)OAc | 47 |
| Chemical etching | MIL-88A | - | PVDF | MIL-88A@PVDF | 48 |
| UV/Vis-lithography | Cu$_3$(BTC)$_2$ | ~ 5 µm | Copper PCB board | - | 49 |

While bottom-up techniques have been used as the main methods to control the spatial location of MOFs on substrates, the top-down technologies are still in their initial stage. For this reason, only a few examples are reported in the literature (see Table 3). Even though several techniques are available, new efforts should be made to develop novel top-down methods that will be suitable for the industry. Photolithography and imprinting processes are presented as promising technologies because of various causes: i) they are compatible with the industrial lithography process, ii) the performance of these techniques is independent on the MOF synthesis methods, and iii) they are very useful to form MOF patterns whose synthesis methods are carried out sometimes under drastic conditions.

Top-down process requires two independent steps: i) MOF deposition over a desired material, and ii) MOF removal from controlled regions. The deposition of MOF films is a well-researched technology that allows to control thin film properties such as thickness, roughness, crystal orientation, porosity and composition.[50,51] The deposition can be accomplished by either i) *in situ* methods, where the MOF synthesis takes place directly onto the substrates, or ii) *ex situ* methods based on the deposition of pre-synthesized MOF

on a given initial material.[52,53] Moreover, numerous materials have been used as substrates, including metals, oxides, polymers, graphene, textile fabrics, depending on the application.[54] In the second step, MOF removal is produced in controlled regions, and consequently the final architecture is achieved. This step is currently based on imprinting and photolithography technologies.

Imprinting technique is a strategy to transfer a given pattern onto a substrate by soft lithography. A patterned stamp is placed in contact with a surface of a malleable material (usually a polymeric material), applying any external pressure and/or heat, if necessary. PDMS is the polymer commonly used as a stamp in soft lithography, because of three advantages: i) it is elastic and ii) transparent down to wavelengths of 280 nm, and iii) it is cheap and commercially available in bulk quantities.[55] Alternatively, other polymers have been used for stamps such as poly(methyl methacrylate) (PMMA), poly([3-mercaptopropyl] methylsiloxane) (PMMS), polystyrene (PS) or epoxy resin.[56] Imprinting methods have been widely employed as patterning technology since they can be used on several substrates like polymers, gels, inorganic carbon, luminescent phosphors, salts or colloids.[56] Nevertheless, this technology has not been routinely applied to MOF-based materials and only a few procedures have been reported to date. An example of imprinting methods for MOF-based materials was provided by Dalstein *et al.*[46] Nanopatterned ZIF-8 and ZIF-8/TiO$_2$ heterostructures with dimensions of 200 nm and different morphology were fabricated by soft-lithography.

In both previous routes, patterned PDMS was used as a stamp and it was fabricated by procedures reported in the literature.[57] In the case of ZIF-8, the polymeric stamp was applied directly on a pre-formed ZIF-8 colloidal suspension. The absorption by capillarity through PDMS allowed the solvent evaporation. Finally, replication of the geometric stamp on the MOF surface was achieved after full evaporation process (Fig. 5). For the ZIF-8/TiO$_2$ heterostructures, a TiO$_2$ film was deposited on a silicon substrate using sol-gel methodology. Once the evaporation of the corresponding solvent resulted, a hard-PDMS stamp was placed over the TiO$_2$ surface, using a degassing assisted patterning strategy.[58] Next, the nanopatterned film was stabilized at 110 ºC for 5 min and ZIF-8 colloids were deposited on it by dip-coating. Finally, the performance as sensors of both structures was demonstrated taking advantage of the variation of optical properties induced by selective adsorption of organic solvent vapours, like isopropanol or styrene/water.
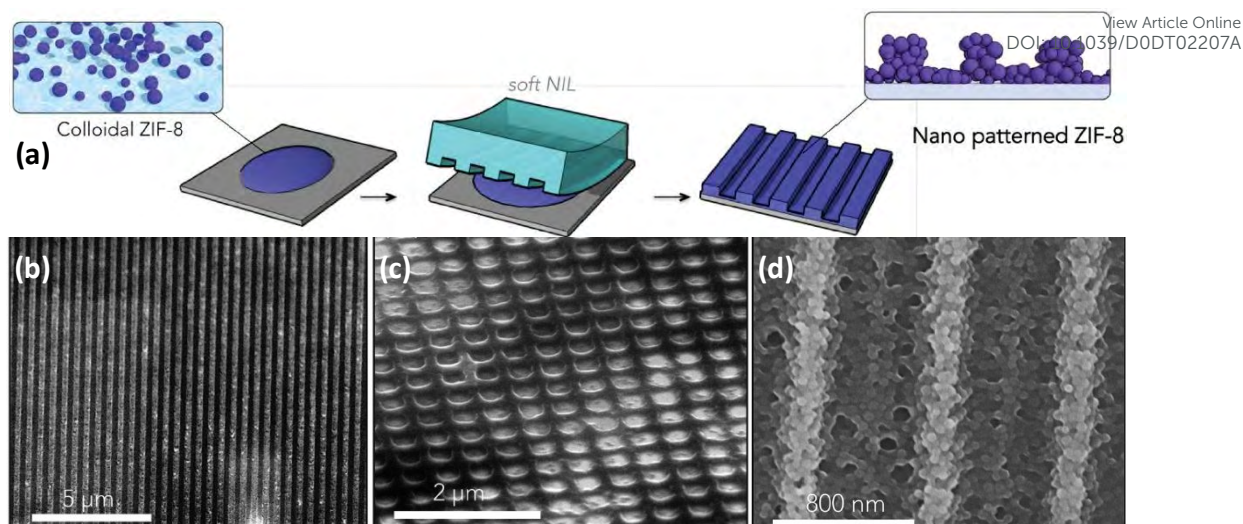
**Fig. 5** a) Synthetic procedure of nanopatterned ZIF-8 by soft nano-imprint lithography (NIL). b) FEG-SEM images of patterned ZIF-8 nanoparticles with square and c) nanogrooves features. d) A higher magnification of b). Reproduced from Ref.[46] with permission from [John Wiley and Sons], copyright [2016].

In addition, PDMS micro-patterns could also be used as moulds to make substrates with similar architectures, which could be useful as supports for MOFs. This has been recently demonstrated by Huang *et al*.[59] The authors performed the correct deposition of UiO-66 on patterned porous yttria-stabilized zirconia (YSZ) ceramic substrates to produce patterned membranes. In addition, they proved that the growth of MOFs in concave areas occurs slower, reducing the average thickness of the membranes. This effect together with the increase of the active area of the membrane contributed to a higher permeation rate and better performance in the butanol dehydration by pervaporation process.

Photolithography has been one of the most common methods used for nanofabrication. Moreover, it has been one of the main top-down techniques used for the production of MOF patterns, although some bottom-up researches have been reported.[60,61] In general, there are three necessary tools to perform photolithography: i) a radiation source, ii) a mask, and iii) a photoresist material. First, a substrate is coated with a photoresist, which can be positive or negative. Next, this assembly is exposed to radiation through a mask with a given geometry (i.e. that has well defined opaque and transparent regions), illuminating the areas of the photoresist covered by the transparent region.[62] When the photoresist is positive, the areas under exposure to photon radiation break down and become more soluble in a developing solution that normally consists of a weak basic solution such as tetramethyl ammonium hydride (TMAH). Alternatively, the exposed

regions of negative photoresist become more stable in a developer. As a result, the photoresist can be removed by an appropriate solvent, and finally a patterned material can be manufactured (Fig. 6).
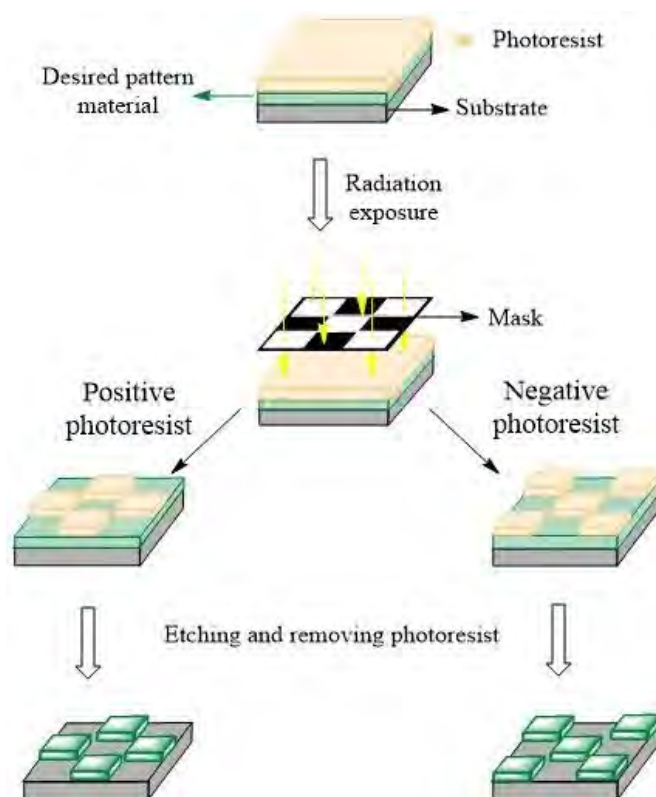


**Fig. 6** Illustrative scheme of a usual procedure to generate patterned material by photolithography.

The UV-lithography, electron beam lithography and X-ray lithography are examples of photolithography techniques, which use different radiation sources to induce a morphology on a photoresist material. These top-down techniques have already been applied to produce patterns in porous materials such as zeolites, and recent efforts have been made to create patterned surfaces of MOFs.[12,63,64] For example, patterning of ZIF-9 over a silicon wafer was elaborated using deep X-ray lithography by Dimitrakakis *et al*.[43] In this work, thin phenyltriethoxysilane (PhTES) films were employed as negative photoresists under X-ray exposure. In the first step, a solution of PhTES was cast on a silicon wafer. After a temperature stabilization, the pre-synthesized particles of ZIF-9 were embedded into the softened PhTES film. This platform was exposed to synchrotron X-ray through a mask. Finally, upon contact with ethanol, the non-irradiated areas were removed and the structures with a resolution of 25 µm and different morphology were successfully developed (Fig. 7).
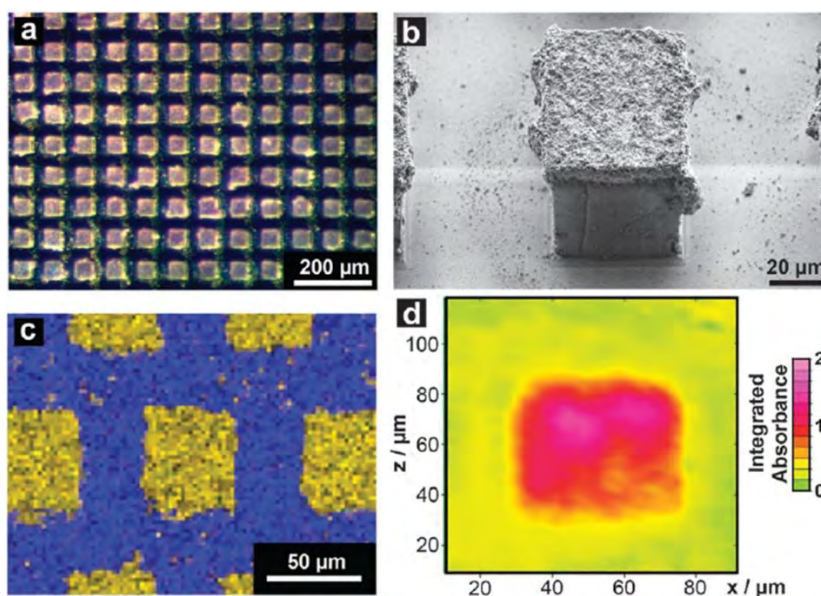
**Fig. 7** Images of the pattern of ZIF-9/PhTES with dimensions of 50 µm x 50 µm: a) imaged optically, b) using SEM, c) with the mapping of the EDX surface silicon (blue) and cobalt (yellow), and d) with the FTIR image of the integrated C-N stretch band characteristic of the ZIF-9. Reproduced from Ref. [43] with permission from [The Royal Society of Chemistry], copyright [2012].

In other research, Conrad *et al*. were able to fabricate patterned MOF-based materials by electron beam induced amorphization on MOF.[47] They showed that some amorphized MOF had greater water stability than its crystalline parent framework, and as a result this MOF could be used as a negative photoresists. The proposed protocol involved a first step to produce MOF films over a substrate: ZIF-L, MIL-101(Cr), ZIF-8 and Zn(BeIm)OAc were deposited on silicon wafers. Next, the selected regions were exposed through a mask using electron beam lithography. After a gentle rinsing in water, only the areas not exposed were removed and a patterned MOF-based material was produced.

UV-lithography has been one of the techniques most employed for MOF patterning. It has reached wide acceptance in the field of microfabrication because of the suitable resolution and greater availability compared to other mentioned techniques. Lu *et al*.[44] developed a protocol for patterning ZIF-8 based on this technique. In this example, a ZIF-8 thin film was deposited on a silicon substrate and then spin-coated with a positive photoresist (AZ1815). To demonstrate the successful pattern of ZIF-8, the platform was exposed to UV radiation through a mask with a given geometry followed by etching and removal of remaining resist. Another alternative approach where UV-lithography was used for MOF patterning was reported by Wang *et al*.[45] In this work, site-selective

**Dalton Transactions Accepted Manuscript**

photoactivation reactions were used to produce MOF patterns with different fluorescent properties. Surface-anchored MOFs (SURMOFs) were applied as photoresist material. It is an emerging topic, due to improved resolution in photolithography technology.[65] Two ways were employed: i) the azide-alkine click reaction and ii) thiol-yne click chemistry. Azide or thiol reactions can be started by UV radiation.[66] It allows them to start the reaction only in the irradiated regions generating patterned MOFs with different chemical structures and properties. Alternately, azide or thiol photodecomposition can be produced by UV energy. It allows SURMOFS to be used as positive or negative photoresist according to the needs. It is important to note that the selected porous photolithography techniques could only be used in robust MOFs from point of view of photostability. To solve this problem, an easy and versatile strategy was implemented by combining imprinting and UV-lithography.[6] In this work, a patterned SU-8 film was fabricated by UV-lithography. $NH_2$-MIL-53(Al), ZIF-8 and ZIF-67 were imprinted over a SU-8 layer, which was previously heated at 95 ºC. Once cooled below its glass transition temperature, a patterned MOF-based material was accomplished. This versatile methodology could be applied to form miniature architectures of all types of MOFs. UV-lithography has been used to activate MIL-88A films prepared on polyvinylidene difluoride (PVDF).

A different top-down technique from the ones previously mentioned was used by Troyano *et al*.[48] The authors developed a homogeneous distribution of MIL-88A embedded in PVDF where they generated a vertical and lateral gradient of the MOFs by chemical etching. This strategy consisted of the controlled exposure of gaseous HCl on the MOF-based material. After exposure, washing and drying, partial removal of MIL-88A in the PVDF was observed. By controlling the exposure zones and time, different patterns such as parallel lines with a thickness of 1 mm were generated. In this work not only the 2D materials were produced but also the reversible transition of these to 3D materials was studied. This is possible due to two causes: i) the property of MIL-88A to swell when it absorbs water, and ii) the formation of the previous patterns that induces the bending of the materials by the zones that do not have MOF, obtaining a 3D structure.

### 3.  Conclusions and outlook

Due to their porosity, crystallinity and organic-inorganic nature, metal organic frameworks (MOFs) are able to crystallize constituting singular structures. Some of these structures are generally ingrown layers that can be patterned with the use of appropriate top down techniques (such as imprinting, photolithography or chemical etching), while

bottom up methodologies can be used to directly obtain patterned structures consisting of nanoparticle agglomerates or single crystals orderly distributed across a certain substrate controlling their, shape, size and surface density. Patterned MOF structures can be also generated upon direct crystallization on a previously patterned supports. In any event, the patterned MOF structures can be found applications in fields dealing with sensors, membranes, catalysis, solar cells, microelectronics, energy saving, pollutant sequestration or optics.

However, some steps forward are needed to reach the complete development of the current MOF patterning methodologies, among them: 1) to find techniques of application to all sort of MOFs, since some of them due to their limited chemical and crystallographic stability cannot withstand the applied conditions so that phase changes can be observed during the patterning process. 2) To access to certain applications, MOF printing techniques should likely decrease their resolution to about 10 nm, as achieved with silicon oxide.[67] 3) Some of the top-down techniques are carried out on MOF coatings with poor intergrowth what can imply, for instance, potential leaks in the generated devices, thus single crystal or like (i.e. better intergrown MOF layers) are needed with the desired dimensions. 4) The patterning techniques should be coupled at the nano and micro scale separation and reaction systems to produce highly integrated and intensified devices able to act in many demanding areas that will suffer a tremendous growth in the next coming years. In fact, this is a great opportunity for MOFs (giving their intrinsic separation and catalytic properties that can be present in a single MOF) not yet fully developed. 5) Finally, as MOFs are of the existing microporous materials those closer to oligomers and polymers in living beings, more inspiration from Nature is probably needed to directly produce MOF based patterned structures from bottom-up approaches.

In conclusion, control of the spatial localization of MOF over different substrates has become a focus of numerous researches. This is due to: i) the excellent properties of MOF such as specific surface, adsorption capacity, flexibility, porosity, organic-inorganic character, and ii) the necessary MOF-substrate coupling in a miniaturized form for advanced applications in microelectronics and sensors. For this reason, it is important to have an overview of the current technologies to create MOF structures with a defined pattern. In this review, the recent state of the art in the use of these methodologies are summarized. However, higher resolution techniques to generate MOF patterns are still in progress and a collaboration from different areas must be made to develop reliable techniques available on an industrial scale. These efforts will lead to the optimization and

industrialization of these techniques that can be useful not only to create a generation of new MOF-based systems but also to design well-defined nanopatterns of different materials.

## References

[1] M. García-Palacín, J. I. Martínez, L. Paseta, A. Deacon, T. Johnson, M. Malankowska, C. Téllez, J. Coronas, *ACS Sustainable Chem. Eng.,* 2020, **8**, 2973–2980.

[2] R. Lin, B. Villacorta Hernandez, L. Ge, Z. Zhu, *J. Mater. Chem. A*, 2018, **6**, 293–312.

[3] X. Jiang, S. Li, S. He, Y. Bai, L. Shao, *J. Mater. Chem. A,* 2018, **6**, 15064–15073.

[4] S. K. Henninger, F. Jeremias, H. Kummer, C. Janiak, *Eur. J. Inorg. Chem.,* 2012, **16**, 2625–2634.

[5] J. Gascon, A. Corma, F. Kapteijn, F. X. Llabrés I Xamena, *ACS Catal.,* 2014, **4**, 361–378.

[6] C. M. Doherty, G. Grenci, R. Riccò, J. I. Mardel, J. Reboul, S. Furukawa, S. Kitagawa, A. J.Hill, P. Falcaro, *Adv. Mater.,* 2013, **25**, 4701–4705.

[7] P. Horcajada, R. Gref, T. Baati, P. K. Allan, G. Maurin, P. Couvreur, G. Férey, R. E. Morris, C. Serre, *Chem. Rev.,* 2012, **112**, 1232–1268.

[8] C. C. Chueh, C. I. Chen, Y. A. Su, H. Konnerth, Y. J. Gu, C. W. Kung, K. C. W. Wu, *J. Mater. Chem. A,* 2019, **7**, 17079–17095.

[9] L. E. Kreno, K. Leong, O. K. Farha, M. Allendorf, R. P. Van Duyne, J. T. Hupp, *Chem. Rev.,* 2012, **112**, 1105–1125.

[10] A. A. Talin, A. Centrone, A. C. Ford, M. E. Foster, V. Stavila, P. Haney, R. A. Kinney, V. Szalai, F. El Gabaly, H. P. Yoon, F. Léonard, M. A. Allendorf, *Science,* 2014, **343**, 66–69.

[11] Y. Cui, Y. Yue, G. Qian, B. Chen, *Chem. Rev,.* 2012, **112**, 1126–1162.

[12] P. Falcaro, R. Ricco, C. M. Doherty, K. Liang, A. J. Hill, M. J. Styles, *Chem. Soc. Rev.,* 2014, **43**, 5513–5560.

[13] L. Sarango, L. Paseta, M. Navarro, B. Zornoza, J. Coronas, *J. Ind. Eng. Chem.,* 2018, **59**, 8–16.

[14] M. Navarro, J. Benito, L. Paseta, I. Gascón, J. Coronas, C. Téllez, *ACS Appl. Mater. Interfaces,* 2018, **10**, 1278–1287.

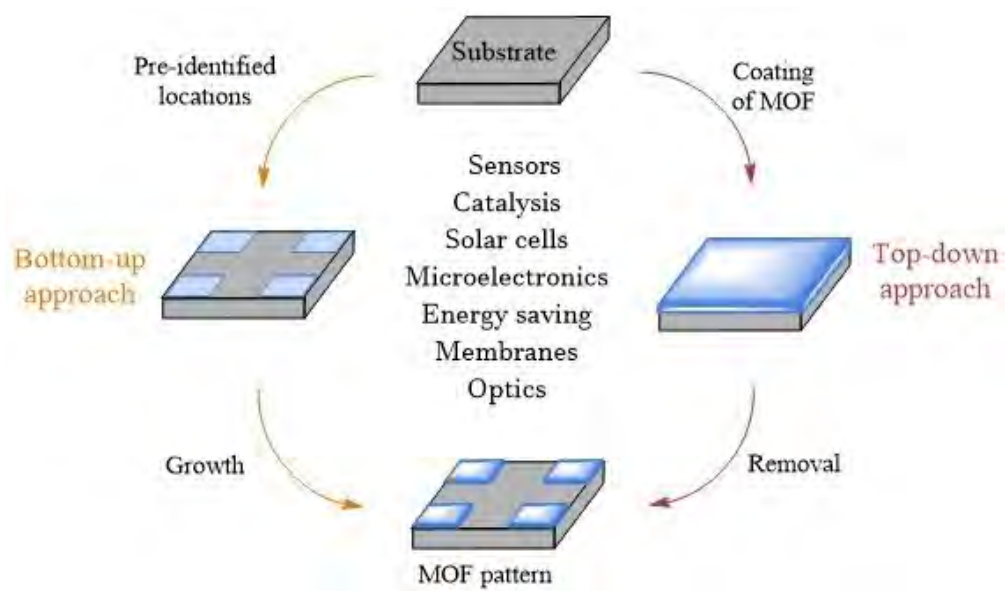[15] J. Liu, C. Wöll, *Chem. Soc. Rev.,* 2017, **46,** 5730–5770.

[16]    K. Jayaramulu, F. Geyer, A. Schneemann, Š. Kment, M. Otyepka, R. Zboril, D. Vollmer, R. A. Fischer, *Adv. Mater.,* 2019, **31**, 1–31.

[17]    B. Liu, M. Ma, D. Zacher, A. Bétard, K. Yusenko, N. Metzler-Nolte, C. Wöll, R. A. Fischer, *J. Am. Chem. Soc.*, 2011, **133**, 1734–1737.

[18]    T. Ladnorg, A. Welle, S. Heißler, C. Wöll, H. Gliemann, *Beilstein J. Nanotechnol.,* 2013, **4**, 638–648.

[19]    D. Witters, N. Vergauwe, R. Ameloot, S. Vermeir, D. De Vos, R. Puers, B. Sels, J. Lammertyn, *Adv. Mater.,* 2012, **24**, 1316–1320.

[20]    R. Ameloot, L. Pandey, M. Van Der Auweraer, L. Alaerts, B. F. Sels, D. E. De Vos, *Chem. Commun.,* 2010, **46**, 3735–3737.

[21]    I. Hod, W. Bury, D. M. Karlin, P. Deria, C. W. Kung, M. J. Katz, M. So, B. Klahr, D. Jin, Y. W. Chung, T. W. Odom, O. K. Farha, J. T. Hupp, *Adv. Mater.,* 2014, **26**, 6295–6300.

[22]    R. Ameloot, E. Cobechiya, H. Uji-i, J. A. Martens, J. Hofkens, L. Alaerts, B. F. Sels, D. E. De Vos, *Adv. Mater.,* 2010, **22**, 2685–2688.

[23]    J. J. Gassensmith, P. M. Erne, W. F. Paxton, C. Valente, J. F. Stoddart, *Langmuir,* 2011, **27**, 1341–1345.

[24]    C. Carbonell, I. Imaz, D. Maspoch, *J. Am. Chem. Soc.,* 2011, **133**, 2144–2147.

[25]    I. Stassen, M. Styles, G. Grenci, H. Van Gorp, W. Vanderlinden, S. De Feyter, P. Falcaro, D. De Vos, P. Vereecken, R. Ameloot, *Nat. Mater.,* 2016*,* **15**, 304–310.

[26]    P. Falcaro, A. J. Hill, K. M. Nairn, J. Jasieniak, J. I. Mardel, T. J. Bastow, S. C. Mayo, M. Gimona, D. Gomez, H. J. Whitfield, R. Riccò, A. Patelli, B. Marmiroli, H. Armenitsch, T. Colson, L. Villanova, D. Buso, *Nat. Commun.,* 2011, **2**, 1-8.

[27]    M. Navarro, B. Seoane, E. Mateo, R. Lahoz, G. F. De La Fuente, J. Coronas, *J. Mater. Chem. A,* 2014, **2**, 11177–11184.

[28]    N. Armon, E. Greenberg, E. Edri, A. Kenigsberg, S. Piperno, O. Kapon, O. Fleker, I. Perelshtein, G. Cohen-Taguri, I. Hod, H. Shpaisman, *Chem. Commun.,* 2019, **55**, 12773–12776.

[29]    H. K. Arslan, O. Shekhah, J. Wohlgemuth, M. Franzreb, R. A. Fischer, C. Wöll, *Adv. Funct. Mater.,* 2011, **21**, 4228–4231.

[30]    J. L. Zhuang, D. Ar, X. J. Yu, J. X. Liu, A. Terfort, *Adv. Mater.,* 2013, **25**, 4631–4635.

[31]    C. H. Su, C. W. Kung, T. H. Chang, H. C. Lu, K. C. Ho, Y. C. Liao, *J. Mater. Chem. A*, 2016, **4**, 11094–11102.

[32]    D. Zacher, R. Schmid, C. Wöll, R. A. Fischer, *Angew. Chem., Int. Ed.,* 2011, **50**, 176–199.

[33]    C. Obermair, M. Kress, A. Wagner, T. Schimmel,  *Beilstein J. Nanotechnol.,* 2012, **3**, 824–830.

[34]    J. Puigmartí-Luis, *Chem. Soc. Rev.,* 2014, **43**, 2253–2271.

[35]    M. Faustini, J. Kim, G. Y. Jeong, J. Y. Kim, H. R. Moon, W. S. Ahn, D. P. Kim, *J. Am. Chem. Soc.,* 2013, **135**, 14619–14626.

[36]    F. Cacho-Bailo, M. Etxeberría-Benavides, O. Karvan, C. Téllez, J. Coronas, *CrystEngComm,* 2017, **19**, 1545–1554.

[37] S. S. Y. Chui, S. M. F. Lo, J. P. H. Charmant, A. G. Orpen, I. D. Williams, *Science,* 1999, **283**, 1148-1150.

[38] M. Li, M. Dincǎ, *Chem. Sci.,* 2014, **5**, 107–111.

[39] T. Stassin, I. Stassen, N. Wauteraerts, A. J. Cruz, M. Kräuter, A. M. Coclite, D. De Vos, R. Ameloot, *Eur. J. Inorg. Chem.,* 2020, **2020**, 71–74.

[40] T. Stassin, S. Rodríguez-Hermida, B. Schrode, A. J. Cruz, F. Carraro, D. Kravchenko, V. Creemers, I. Stassen, T. Hauffman, D. De Vos, P. Falcaro, R. Resel, R. Ameloot, *Chem. Commun.,* 2019, **55**, 10056–10059.

[41] J. Gascon, S. Aguado, F. Kapteijn, *Microporous Mesoporous Mater.,* 2008, **113**, 132–138.

[42] R. Ranjan, M. Tsapatsis, *Chem. Mater.,* 2009, **21**, 4920–4924.

[43] C. Dimitrakakis, B. Marmiroli, H. Amenitsch, L. Malfatti, P. Innocenzi, G. Grenci, L. Vaccari, A. J. Hill, B. P. Ladewig, M. R. Hill, P. Falcaro, *Chem. Commun.,* 2012, **48**, 7483–7485.

[44] L G. Lu, O. K. Farha, W. Zhang, F. Huo, J. T. Hupp, *Adv. Mater.*, 2012, **24**, 3970–3974.

[45] Z.Wang, J. Liu, S. Grosjean, D. Wagner, W. Guo, Z. Gu, L. Heinke, H. Gliemann, S. Bräse, C. Wöll, *ChemNanoMat,* 2015, **1**, 338–345.

[46] O. Dalstein, D. R. Ceratti, C. Boissière, D. Grosso, A. Cattoni, M. Faustini, *Adv. Funct. Mater.,* 2016, **26**, 81–90.

[47] S. Conrad, P. Kumar, F. Xue, L. Ren, S. Henning, C. Xiao, K. A. Mkhoyan, M. Tsapatsis, *Angew. Chem., Int. Ed.,* 2018, **57**, 13592–13597.

[48] J. Troyano, A. Carné-Sánchez, D. Maspoch, *Adv. Mater.*, 2019, **31**, 1–7.

[49] K. Okada, R. Ricco, Y. Tokudome, M. J. Styles, A. J. Hill, M. Takahashi, P. Falcaro, *Adv. Funct. Mater.,* 2014, **24**, 1969–1977.

[50] J. L. Zhuang, A. Terfort, C. Wöll, *Coord. Chem. Rev.,* 2016, **307**, 391–424.

[51] I. Stassen, N. Burtch, A. Talin, P. Falcaro, M. Allendorf, R. Ameloot, *Chem. Soc. Rev.*, 2017, **46**, 3185–3241.

[52] V. Stavila, A. A. Talin, M. D. Allendorf, *Chem. Soc. Rev.,* 2014, **43**, 5994–6010.

[53] Y. Han, P. Qi, X. Feng, S. Li, X. Fu, H. Li, Y. Chen, J. Zhou, X. Li, B. Wang, *ACS Appl. Mater. Interfaces,* 2015, **7**, 2178–2182.

[54] A. Bétard, R. A. Fischer, *Chem. Rev.,* 2012, **112**, 1055–1083.

[55] M. P. Wolf, G. B. Salieb-Beugelaar, P. Hunziker, *Prog. Polym. Sci.,* 2018, **83**, 97–134.

[56] K. Matyjaszewski, in *Polymer Science: A Comprehensive Reference*, D. J. Lipomi, R. V. Martinez, L. Cademartiri, G. M. Whitesides, Elsevier, 1, 2012, 7.11, 211-231.

[57] A. Cattoni, E. Cambril, D. Decanini, G. Faini, A. M. Haghiri-Gosnet, *Microelectron. Eng.,* 2010, **87**, 1015–1018.

[58] C. Luo, X. Ni, L. Liu, S. I. M. Nomura, Y. Chen, *Biotechnol. Bioeng.*, 2010, **105**, 854–859.

[59] K. Huang, B. Wang, S. Guo, K. Li,. *Angew. Chemie - Int. Ed.,* 2018, **57**, 13892–13896.

[60] T. Tsuruoka, T. Matsuyama, A. Miyanaga, T. Ohhashi, Y. Takashima, K. Akamatsu, *RSC*

*Adv.,* 2016, **6**, 77297–77300.

[61]   B. K. Keitz, C. J. Yu, J. R. Long, R. Ameloot, *Angew. Chem., Int. Ed.,* 2014, **53**, 5561–5565.

[62]   T. Betancourt, L. Brannon-Peppas, *Int. J. Nanomed.,* 2006, **1**, 483–495.

[63]   S. K. Kirdeciler, C. Ozen, B. Akata, *Microporous Mesoporous Mater.,* 2014, **191**, 59–66.

[64]   V. Tsukala, D. Kouzoudis, *Microporous Mesoporous Mater.,* 2014, **197**, 213–220.

[65]   M. Drost, F. Tu, L. Berger, C. Preischl, W. Zhou, H. Gliemann, C. Wöll, H. Marbach, *ACS Nano,* 2018, **12**, 3825–3835.

[66]   R. T. Chen, S. Marchesan, R. A. Evans, K. E. Styan, G. K. Such, A. Postma, K. M. McLean, B. W. Muir, F. Caruso, *Biomacromolecules,* 2012, **13**, 889–895.

[67]   M. Graczyk, A. Cattoni, B. Rösner, G. Seniutinas, A. Löfstrand, A. Kvennefors, D. Mailly, C. David, I. Maximov, *Microelectron. Eng.,* 2018, **190**, 73-78.

21

150x88mm (96 x 96 DPI)